AD_____

Award Number: DAMD17-00-1-0195

TITLE: Tactile Mapping of Breast Palpation for Diagnosis,
Documentation, and Training

PRINCIPAL INVESTIGATOR: Rujirutana A. Srikanchana

CONTRACTING ORGANIZATION: The Catholic University of America
                           Washington, DC 20064

REPORT DATE: September 2001

TYPE OF REPORT: Annual Summary

PREPARED FOR: U.S. Army Medical Research and Materiel Command
               Fort Detrick, Maryland 21702-5012

DISTRIBUTION STATEMENT: Approved for Public Release;
                        Distribution Unlimited

The views, opinions and/or findings contained in this report are
those of the author(s) and should not be construed as an official
Department of the Army position, policy or decision unless so
designated by other documentation.

REPORT DOCUMENTATION PAGE

Public reporting burden for this collection of information is estimated to average 1 hour per response, including the time for reviewing instructions, searching existing data sources, gathering and maintaining the data needed, and completing and reviewing this collection of information. Send comments regarding this burden estimate or any other aspect of this collection of information, including suggestions for reducing this burden to Washington Headquarters Services, Directorate for Information Operations and Reports, 1215 Jefferson Davis Highway, Suite 1204, Arlington, VA 22202-4302, and to the Office of Management and Budget, Paperwork Reduction Project (0704-0188), Washington, DC 20503

1. AGENCY USE ONLY (Leave blank)	2. REPORT DATE September 2001	3. REPORT TYPE AND DATES COVERED Annual Summary (1 Sep 00 - 31 Aug 01)

4. TITLE AND SUBTITLE
Tactile Mapping of Breast Palpation for Diagnosis, Documentation, and Training

5. FUNDING NUMBERS
DAMD17-00-1-0195

6. AUTHOR(S)
Rujirutana A. Srikanchana

7. PERFORMING ORGANIZATION NAME(S) AND ADDRESS(ES)

The Catholic University of America
Washington, DC 20064

E-Mail: 55srikan@pluto.ee.cua.edu

8. PERFORMING ORGANIZATION REPORT NUMBER

9. SPONSORING / MONITORING AGENCY NAME(S) AND ADDRESS(ES)

U.S. Army Medical Research and Materiel Command
Fort Detrick, Maryland 21702-5012

10. SPONSORING / MONITORING AGENCY REPORT NUMBER

11. SUPPLEMENTARY NOTES

12a. DISTRIBUTION / AVAILABILITY STATEMENT
Approved for Public Release; Distribution Unlimited

12b. DISTRIBUTION CODE

13. Abstract (Maximum 200 Words) (abstract should contain no proprietary or confidential information)

Breast palpation by clinicians is an effective examination frequently performed for breast cancer detection and treatment monitoring. The utilization of physical breast examination however has been hampered by its inherent subjective nature leading to (1) the difficulty in interpreting the examiner's impressions of the perceived lump in the breast and (2) the difficulty in documenting tactile characteristics of the tumor for subsequent examinations or monitoring. Based on the preliminary studies funded by an NCI grant award, the primary objective of this predoctoral training project is to advance an effective *tactile mapping device* (TMD) for a quantitative and objective characterization of breast cancer through breast palpation, showing that the TMD will improve physical breast examination in the ability to characterize tumor's biomechanics and increase the efficacy of early detection and treatment monitoring, thus leading to improved diagnosis and a reduction in breast cancer mortality. An equally important objective is to acquire a solid training for the trainee to gain experience necessary for developing a research career in breast cancer research.

14. SUBJECT TERMS
Breast Examination, cancer detection, treatment monitoring, tactile Imaging, neural networks, telemedicine

15. NUMBER OF PAGES
31

16. PRICE CODE

17. SECURITY CLASSIFICATION OF REPORT Unclassified	18. SECURITY CLASSIFICATION OF THIS PAGE Unclassified	19. SECURITY CLASSIFICATION OF ABSTRACT Unclassified	20. LIMITATION OF ABSTRACT Unlimited

NSN 7540-01-280-5500

Standard Form 298 (Rev. 2-89)
Prescribed by ANSI Std. Z39-18
298-102

Table of Contents

INTRODUCTION

Breast palpation by clinicians is an effective examination frequently performed for breast cancer detection and treatment monitoring. The utilization of physical breast examination however has been hampered by its inherent subjective nature leading to (1) the difficulty in interpreting the examiner's impressions of the perceived lump in the breast and (2) the difficulty in documenting tactile characteristics of the tumor for subsequent examinations or monitoring. The primary objective of the Task I is to adapt new tactile sensing technologies to the needs of improving physical breast examination and gather preliminary data regarding potential clinical applications. A novel and effective *tactile mapping device* (TMD) has been developed to quantitatively characterize breast cancer through breast palpation so as to demonstrate the feasibility and effectiveness of the TMD to the three specific applications: diagnosis, documentation, and training. Limited laboratory experimental evaluation has been conducted to collect preliminary data that will permit formation of a full-scale Task II research plan. Our considerable efforts in the Task I are

- Transfer and adapt the existing tactile sensor array and force measurement technologies for robotics application to medical sensing application.
- Modify the design specifications of tactile sensor array construction for the specific application of TMD in breast palpation.
- Apply TMD to various educational breast models and in-house phantoms (with various lumps within the models) to collect sufficient tactile images.

BODY

Following the tasked research plan, the development of a prototype TMD comprised mainly of a tactile sensor array probe (TSAP) [7,15,30], a 3D camera [6,9], a 6 degree-of-freedom (DOF) force/torque sensor [7,14,33], and a graphical user interface [7], which can provide the means to produce tactile maps of the detected breast lumps during a breast palpation. Focusing on the key tactile topology features from breast palpation such as spatial location, size and shape of the detected lesion, and the force levels used to demonstrate the palpable abnormalities, these maps can record the results of clinical physical breast examination with a set of pressure distribution profiles (i.e., images) due to detected lesion and the force sensor measurements corresponding to the applied force levels. These maps will serve as an objective documentation of palpable lesions for subsequent examinations and/or follow-up treatment assessment. Using advanced signal processing techniques, these maps will also provide new information for characterization of tumor biomechanics [8,18]. Preliminary results of simulated experiments of the TMD prototype have pilot-tested our hypothesis and provided solid promising data showing the feasibility of the TMD in real clinical applications [7,8,9].

We have conducted a systematic study to adapt new tactile sensing technologies to the needs of improving physical breast examination, to gather preliminary data regarding potential clinical applications, and to advance fundamental understanding of palpation. Using the prototype TMD, we have measured three key variables during palpation: the examiner's search patterns, the applied forces, and the small-scale pressure variations at the skin due to lumps, and have conducted intensive experimental studies evaluate its performance. The primary objective aims that (1) new tactile mapping technology can quantitatively measure the location and applied forces in breast palpation, and the tactile features of detected breast lumps; and (2) new device can accurately characterize and document breast lumps and will improve clinicians' ability to monitor changes in lump across time. We have also calibrated and pilot tested the prototype TMD through laboratory experiments to evaluate TMD's performance in terms of reliability, validity, and safety. Our experiment has shown that this novel TMD system can make it possible to quantitatively and objectively record and characterize the processes and findings of breast palpation.
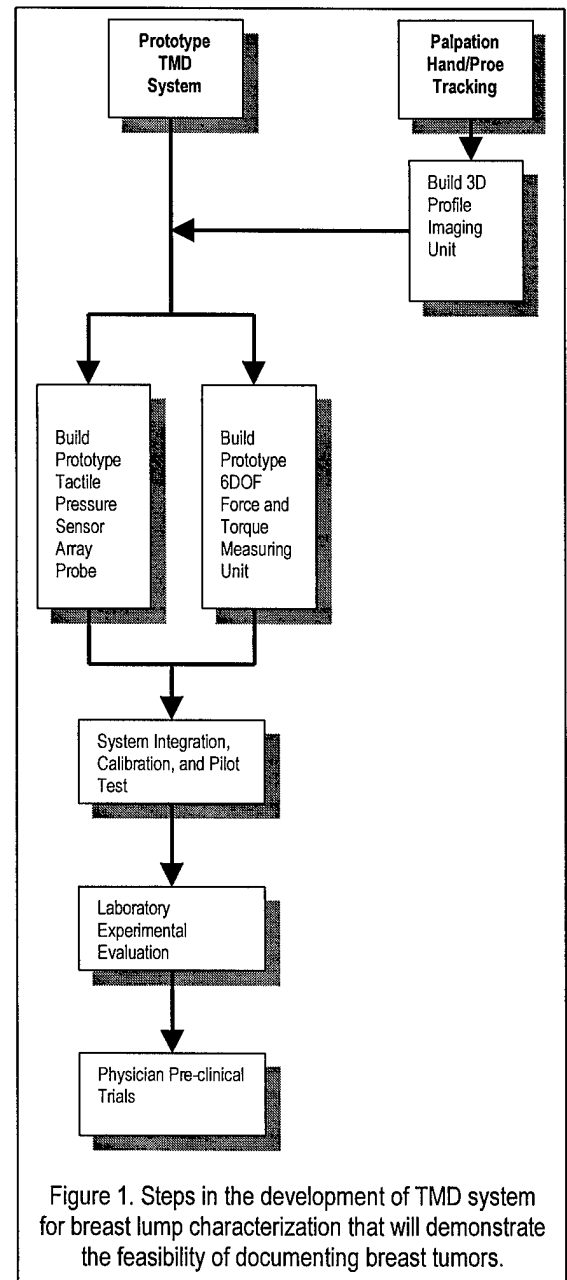

Figure 1. Steps in the development of TMD system for breast lump characterization that will demonstrate the feasibility of documenting breast tumors.

System Overview

The goal of this prototype TMD system is to extend the range and resolution of breast palpation methods, thus increasing palpation sensitivity and specificity (i.e, the ability to detect and characterize lumps and quantify clinically significant changes). Using 3D camera, force sensor, and tactile sensor arrays, we can create reproducible tactile maps (or images) of the palpable abnormalities in the breast. With various sizes and resolution of the tactile sensor arrays, the TMD can record the multi-foci spatial distribution of the detected lumps and the higher resolution tactile images of a particular lump.

Our prototype TMD system incorporates a 3D Rainbow camera, a tactile sensor array probe (TSAP), a breast model with simulated lumps, a 6DOF force/torque sensor on which the breast model is mounted, and a graphical user interface (GUI). Figure 2 shows a block diagram of the prototype *tactile mapping device* system being developed for measurement and

2

characterization of palpable abnormalities in the breast in a laboratory setting and later in pre-clinical trial. In a typical task, upon detecting a suspicious lump with a lower tactile perception threshold, the examiner will bring the TSAP into contact with the tissue at the palpation site. For a thorough tactile mapping procedure, this involves 3D positioning the probe through the camera facing the site. The resulting pressure distribution across the probe surface is measured by a tactile sensor array with associated readout electronics. Multiple tactile images with various applied force levels and torque angles will be required for an accurate lesion characterization. A computer will process and control the signals to generate appropriate output for visual display on a monitor as an interactive feedback to the on-line users or the raw data to the physician's office through a telecommunication channel. This prototype TMD system was successfully developed and has been working effectively and reliably in our research site. Through extensive testing and physician's inspection (by Dr. Matthew Freedman), we believe that our prototype TMD has fully achieved the design objective [7]. Below, we describe the components of the TMD prototype in detail.

Figure 2. System block diagram of prototype TMD.
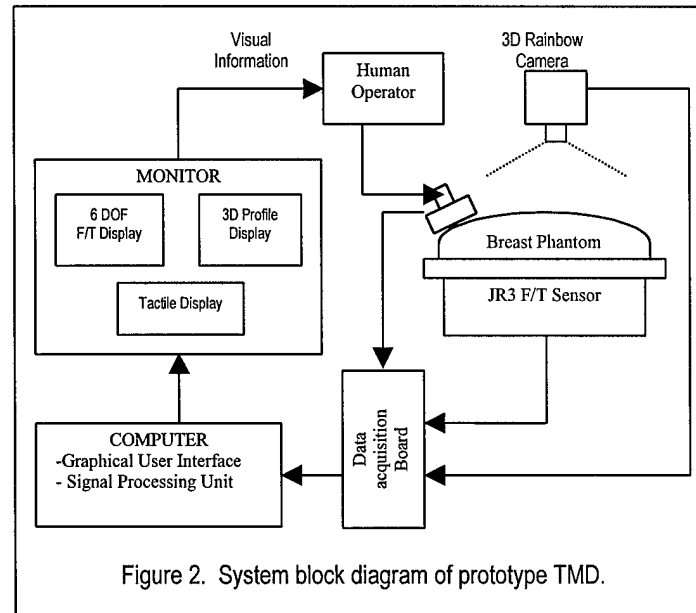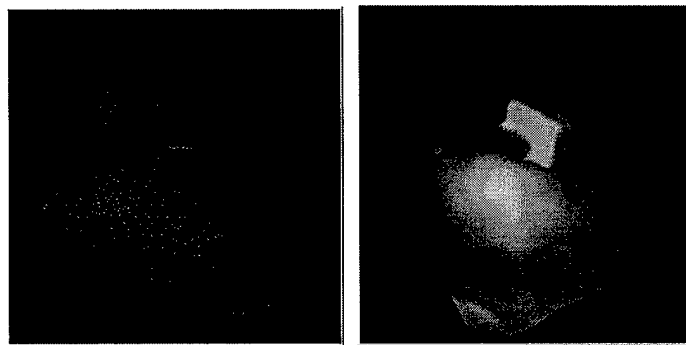
3D Rainbow Camera

Figure 3. 3D range imaging of palpation tracking by the Rainbow camera.

For the accurate positioning of the TSAP with the purpose of tumor localization, a novel 3D rainbow camera is adopted in our system, which is suitable for this high-speed 3D machine vision application. Figure 3 shows the rainbow camera acquired sample 3D range image of breast palpation procedure, where the examiner's hand/fingers, TSAP, and breast profile are clearly identified. It exploits a color light projector to illuminate the object in the scene and using an off-the-shelve color camera to obtain a full-frame color image of the scene. The color of the projecting light with spatially continuously varying wavelength is encoded with information of the corresponding projection angle. Each pixel of the color image is associated with a unique ray through the focal point of the camera. Since the angle between camera axis and the ray is known, the resulting angle-side-angle triangulation problem can be precisely solved when the distance

3

between the light projector and the camera is fixed. Thus, using only one camera, the full frames of 3D range images can be obtained directly at the camera frame rate (60 frames/s). We have performed experiments to investigate the actual range accuracy and the major error contributors. The results show that the 3D profiles of test artifacts were less than 1 mm. The spatial resolution of the system is limited only by the spatial resolution of the camera optical sensing element and is currently able to provide at least 1024x1024 pixel resolution. When a palpation site is determined, multiple 3D range images will be acquired to record the site information [6,9].

Tactile Sensor Array Probe (TSAP)

The core component of the TMD is a high sensitive tactile sensor array probe. A signal acquisition and processing unit with specifically designed software and hardware components have been developed to generate high signal-to-noise ratio tactile readout images. Though many other types of tactile sensors are available, we have decided to use a capacitive tactile sensor in this application since it has been well tested in surgical applications such as minimally invasive surgery and is the state-of-the-art technology in this domain [14,17,28,19]. The actual tactile sensor array with the copper layers and the silicone rubber spacers, which is based on the state-of-the-art design by our consultant Fearing [15,30,34] and former collaborator Howe [17,28]. The array is composed of two crossed layers of copper strips separated by thin strips of silicone rubber [15,17]. Each crossing area forms a capacitor, and when a force is applied onto where the strips cross, the distance between the strips decreases and the capacitance increases [28,30]. Specially designed electronics will measure the capacitance of each element and relate the capacitance change to the force applied to each element. By measuring the capacitance variations from all the elements simultaneously, we can determine the spatial distribution of pressure across the sensor array. The sensor array is made with an inexpensive photolithography and an etching process and can be easily attached to a variety of probe shapes. In this prototype specification, it is composed of an eight by eight-tactile sensor array with elements that are 4 mm on a side. The sensor is mounted on a plastic brass backing plate with a surface that has been machined into a section of a square. The backing plate is 5.08 cm on a side and the effective sensing area is 3.20 cm on a side. We decided to make the sensor flat in order to minimize inhomogeneity because the resulting pressure distribution should have a uniform overall signal to noise ratio. The tactile images will then be consistent when used for various breast/chest background textures. Other shapes of the TSAP are undergoing investigation. The actual spatial resolution of the tactile sensor array is 4 mm long where the smallest masses that we are currently interested to characterize are on the order of 1 cm in diameter. Smaller elements would increase spatial resolution at the cost of lower coverage area and low sensitivity since the capacitance is proportional to the element area [28,30]. The tactile sensor has been shielded to provide electronic insulation.

Force/Torque Sensing System

The relationship between the hard inclusion (i.e., lump) and the perceived tactile image from the TSAP is nonlinear and complex. In order to characterize and later extract the tactile features of the detected breast lumps, the TMD operation requires that the force/torque levels exerted by the operator on the breast model be measured together with the corresponding tactile images. It would be ideal if a force/torque sensor were to be mounted between the wrist and the hand of the operator. Since it may be problematic and impractical to mount a force/torque sensor in such a configuration for the prototype system, we decided to mount it under a base, which the breast model is placed on. The force/torque levels acquired by the sensor in this configuration can be transformed to those exerted by the operator via proper coordinate transformation where the applied forces and angles are two important parameters. The JR[3] force/torque sensor mainly consists of a JR[3] monolithic six DOF force sensor and a JR[3] Intelligent Support System[TM], comprised of boards for signal conditioning, data acquisition and processing. A computer program was written in Visual C[++] to send control command to request the JR[3] force/torque sensing unit to send the measurement values to the computer including six force/torque levels and the Cartesian x-, y-, z-axes assigned to the base. The transmitting and receiving of data between the computer and the force/torque system is carried out through serial port. We have conducted laboratory experiments to evaluate the sensitivity of the force/torque system. The preliminary data indicated that the force measurement sensitivity is ± 0.01 lb with a maximum value of 5 lb. Through physician's pre-clinical trials (by Dr. Matthew Freedman), the sensitivity and maximum load are suitable to the desired task.

Breast Models

The breast models used in our laboratory experiments were provided by the HEALTH EDCO, a Division of WRS Group, Inc. and the Mammatech, Co. The models were made from BIOLIKE™ synthetic tissue that feels just like a real breast [13,25]. Two models were used in our tests to collect preliminary data. Each of them has 5 lumps that simulate easy- and hard-to-find breast tumors with various sizes and depths at different locations. One of the models is the geriatric breast that is ideally shaped to address the special problems of older women. The geriatric model simulates the natural stretching of the tissue with age. Figure 4 shows the breast model and the distribution of simulated lumps (lesions) in the breast model respectively. Physician's inspections have shown that the breast models are well suitable for laboratory experiment to gather preliminary data. It should be noticed that as high as 50% of breast cancers occur at the axilia area which is difficult to imaging.
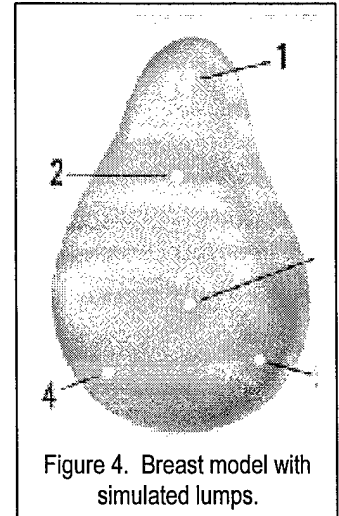

Figure 4. Breast model with simulated lumps.
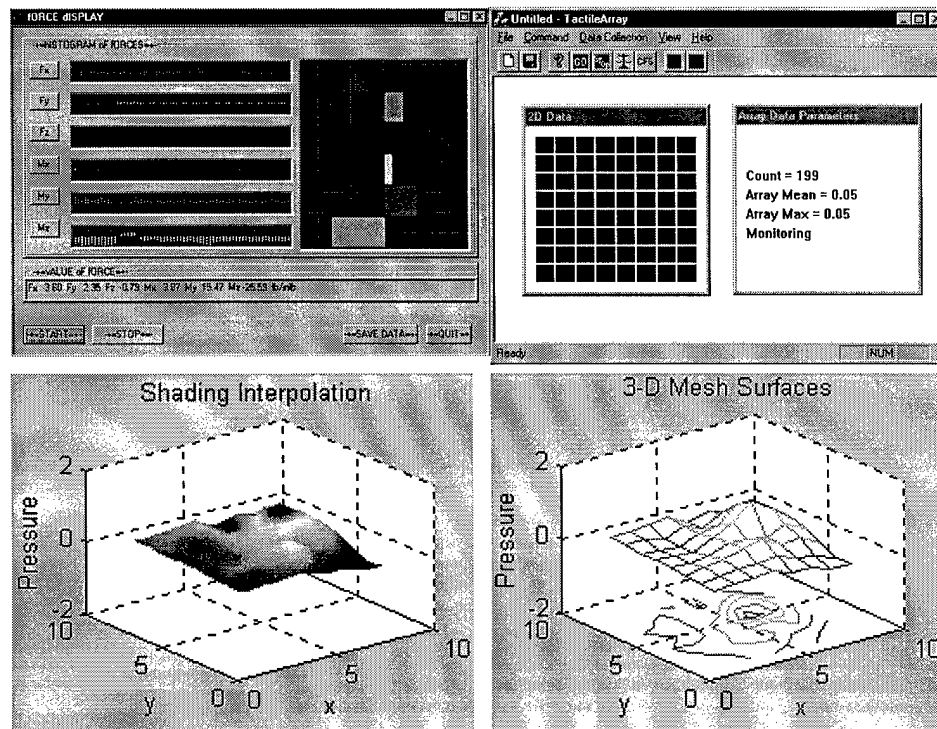
Graphical User Interface

Figure 5. Graphical user interface (GUI) of the TMD prototype including 6DOF force/torque feedback (up-left), tactile imaging control menu (up-right), visual display of pressure distribution (down-left), and 3D mesh and contour map based localization (down-right).
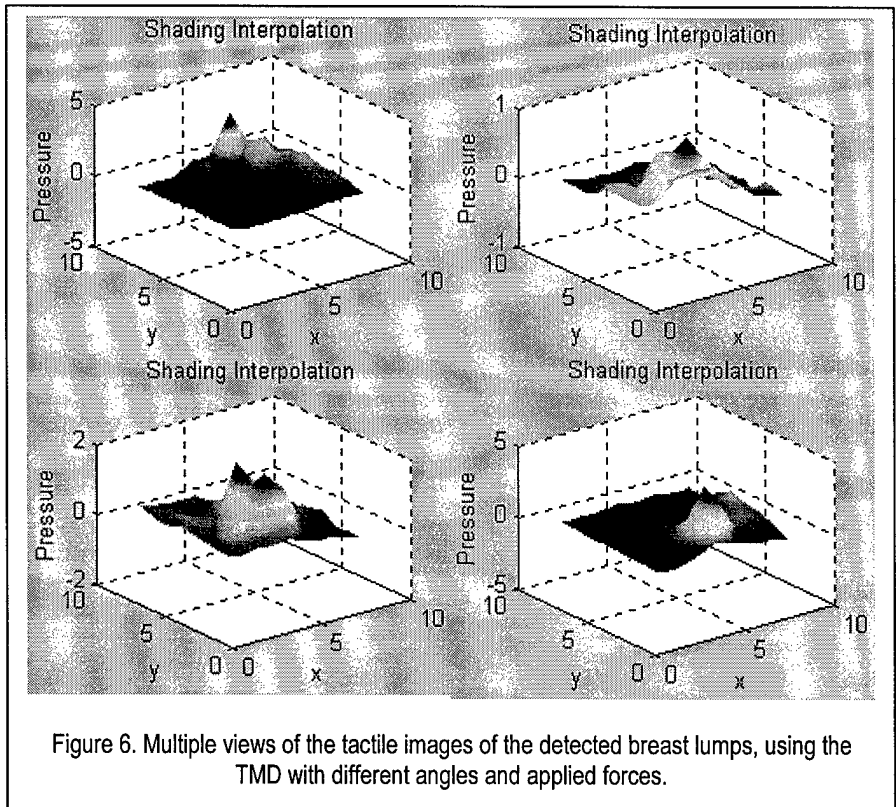
For both tactile documentation and interactive training, a graphical user interface (GUI) plays a very important role of optimizing both machine and examiner's performance. Since such kind of GUI has not been available previously, we have put considerable effort to develop this function. The difficult issue here is that the GUI needs to integrate three different functions (tactile sensing, force sensing, and visual display, which were previously developed in different platform (DOS and Window95), and language (C^{++}, Assembly, and Matlab). In our prototype system, Microsoft Visual C^{++} was employed to implement the GUI to visually display pertinent data of the TSAP and the force/torque sensor. Figure 5 shows the output window of the GUI that presents on-line the pressure distribution acquired by the TSAP, the time response of the six DOF force/torque applied by the examiner. The user can use mouse to interact with the TMD functions through the specifically designed menu.

5

Applications in Documentation

Using the prototype TMD, we have generated various tactile images of the detected breast lumps as an objective electronic document for lesion characterization in subsequent examinations. We have evaluated the performance of the TMD in this application in terms of reproducibility for subsequent exams and for different users regarding key tactile features such as pressure profiles and applied forces. The preliminary data have clearly shown the effectiveness and feasibility of tactile mapping in understanding and improving physical breast examinations for breast cancer diagnosis. Through statistical data analysis and physician's pre-clinical inspection, the reproducibility, sensitivity, and specificity were very satisfactory.

In order to demonstrate the effectiveness of the TMD system for the characterization and documentation of detected lumps, intensive experiments

Figure 6. Multiple views of the tactile images of the detected breast lumps, using the TMD with different angles and applied forces.

have been conducted to pilot-test the sensitivity and reproducibility of the system in measuring the applied forces and the pressure profiles due to lumps. The primary objective here is to quantitatively acquire tactile measurements of the perceived lesions using the TMD system and to evaluate the performance of the system. In a typical experiment described below, the force/torque levels applied by the human examiner during palpation process are recorded in terms of six force/torque parameter values, i.e., F_x, F_y, F_z, M_x, M_y, M_z. For the tactile imaging of simulated lesions, the TSAP is used to acquire various tactile images by palpating the site after the examiner locates the lesion by initial hand palpation with lower tactile perception threshold. Since the relationships between the tactile images and lesion characteristics are expected to be complex and nonlinear, we believe that the inverse problem (extraction of lesion characteristics from tactile images) can be solved when sufficient tactile information is acquired. As a result, for each of the lesions, after pushing the TSAP against the breast to achieve certain level of force, the examiner rotates the TSAP to five different orientations at each of which the information about the force/torque levels and tactile image are simultaneously recorded. OR1 is the initial orientation of the TSAP after being pushed by the examiner to certain level of force. OR2, OR3, OR4 and OR5 are the TSAP orientations after it is rotated forward, backward, left and right, respectively.

We have carried out the above procedure on a total of 10 simulated lesions within two types of breast models with each of them containing five lesion clusters numbered from 1 to 5. Our experience has indicated that the TMD had a high sensitivity for the detection of lesions #1, #4, and #5, while had a difficulty to detect lesions #2 and #3 confidently. We believe that these data has also supported the TMD's complementary role to the mammography. Therefore, by focusing on those suitable lesions, a total of six sets of tactile maps have been generated with each of them containing five tactile images. Figure 6 shows several typical tactile images where two representative lesions (#1 and #4) were studied. A shading interpolation of the pressure distribution measured by the TSAP has been employed to achieve better visual perception. These tactile images have for the first time quantitatively displayed the tactile features of the lumps during breast palpation.

Lesion	TSAP Orientation	6DOF Force & Torque (lb/inlb)					
		Fx	Fy	Fz	Mx	My	Mz
1	OR1	-0.89	0.44	-0.13	-2.58	-10.80	0.50
	OR2	-2.34	2.50	-0.10	-5.26	-22.02	1.59
	OR3	1.69	2.96	-0.03	-2.28	-10.50	3.57
	OR4	3.20	-0.38	0.27	0.40	0.40	2.09
	OR5	-1.83	0.38	-0.03	-2.38	-9.32	1.99
4	OR1	-3.17	1.77	-0.16	5.85	25.59	-0.89
	OR2	-2.08	2.48	-0.22	4.37	18.35	1.78
	OR3	-8.81	-0.03	-0.09	1.98	10.71	0.20
	OR4	-3.67	-1.72	0.00	2.18	10.01	0.39
	OR5	-4.77	4.02	-0.34	2.18	10.81	3.97

The above table summarized the values of force/torque levels recorded from the experiments that were conducted to map the Lesions #1 and #4. Before conducting the experiment on Lesion #1 and Lesion #4, we apply the same procedure on a location at which there exists no lesion, as the fully controlled cases. The resulting display shows no peak. Examining the graphical displays in Figure 6, in comparison with that of the case of no lesion, we noticed that pressure peaks consistently occur in the display and a peak in the graphical display indicates the existence of a corresponding lesion. Our experience has also shown that there is a trade-off between the actual spatial resolution and the signal-to-noise ratio (SNR). Thus, further optimization of the TSAP is needed and should be under the guidance of experimental data showing the best tactile characterization of various lumps. In addition, the force and torque levels that we recorded in conjunction with the tactile sensing during palpation will provide us the information about the contact location and how much force that we apply on the hard lump in the breast model. We have repeatedly conducted documentation experiments at different times, applied to different lesions, and by different users in the past six months. Our intensive results have consistently shown the excellent reproducibility of the prototype TMD where the mean squared error (MSE) was used to measure the different between two tactile images acquired by the TMD for two identical settings. Preliminary statistical analysis also indicated the variance of the experimental data (tactile profile, force, and 3D location) is small.

Applications in Training

We have studied the feasibility of TMD for training of examiners in performing physical breast examination, through the integration of a computerized interactive training system, with the purpose of improving the trainees' ability in how best to search palpable abnormalities with optimal forces in detecting smaller tumors. More specifically, 3D range imaging will track the hand motion and calculate the total coverage of the palpation, and 6DOF force/torque sensor will measure the applied forces and directions. The GUI will provide the trainee a visual feedback of those measured parameters so that this interactive training program can help the trainee to understand the principal of breast palpation and adjust/improve his/her skills.

We have developed a vision-based finger motion tracking technique to gather spatial finger-position related data and have pilot tested this prototype system for breast palpation training using this technique [9]. By tracking the position of the fingers, the system can provide first-hand quantitative data about the search patterns of the palpation process. By displaying position information in real time as the palpation is performed, the system can provide for the first time the feedback so that the trainee can self check his/her search strategy and instantly know which areas have been covered. While other object tracking techniques (e.g., magnetic or acoustic) have been proposed, vision-based tracking is considered to be the most appropriate to our task because it is the least obstructive and expensive method. Using our 3D range camera, we have adopted a model-based approach in which a 3D model of a generic human hand were employed and fitted to the specific hand shape of the user for tracking hand motion. In order to reduce the complexity of the approach, we have developed a color-assisted finger tracking step which tracks the 2D spatial positions of the three colored palpation fingernails during the training procedure. Color transform is utilized to extract color features instead of directly using the RGB values. Normalization of color attributes is used to tackle the problem of potential minor ambient lighting variations.

We have implemented a prototype palpation-training program based on the proposed finger tracking and force/torque sensing approach. A small-scale database has been collected from the recorded expert's palpation experience. Three parameters of visual feedback are provided to the trainee: (1) search pattern, (2) applied force level, and (3) coverage area. The system has been tested in a laboratory setting. The preliminary experimental results have proven reliable and accurate performance in tracking finger positions in 3D and the corresponding applied force levels.

A major portion of the work was reported in our recent manuscript submitted to the *VACETS Technical International Conference* [Attached].

KEY RESEARCH ACCOMPLISHMENTS

Our key research of the Task I is to develop a TMD with various resolutions and sizes to quantitatively document the locations and extract the tactile features of the detected breast lumps. Our accomplishments in the Task I are the following

- *Prototype System Development*: We have developed, calibrated, and pilot tested a novel TMD by integrating state-of-the-art tactile pressure sensor, force/torque sensor, and 3D visual tracking technologies, and conducted laboratory experiments and limited pre-clinical trial to evaluate TMD's performance in terms of reliability, validity, and safety.

- *Application in Documentation*: We have applied TMD to generate the tactile images of the detected breast lumps for a quantitative and objectively characterization of breast cancers in subsequent examinations, and evaluated TMD's performance in improving diagnosis in terms of reproducibility, sensitivity, and specificity for different cases/users/exams.

- *Application in Training*: We have studied the feasibility of TMD for training of examiners in performing physical breast examination, through the integration of a computerized interactive training system, with the purpose of improving the trainees' ability in how best to search palpable abnormalities with optimal forces in detecting smaller tumors.

REPORTABLE OUTCOMES

- Research training under Dr. Robert Wagner supervision at Center of Devices and Radiological Health (FDA). Evaluating diagnosis performance and uncertainty of mutimodalities using Receiver Operating Characteristics (ROC) analysis without knowing the truth.

- Non-Rigid Image Registration by Neural Computations, R. Srikanchana, K. Woods, J. Xuan, C. Nguyen, and Y. Wang, *Proceedings of IEEE Neural Networks for Signal Processing*, 2001.

- Tactile Mapping of Palpable for Breast Cancer Diagnosis, R. Srikanchana, C. Nguyen, and Y. Wang, *VACETS Technical International Conference*, 2001.

- Presented the paper "Non-Rigid Image Registration by Neural Computations", *Conference of IEEE Neural Networks for Signal Processing*, Falmouth, MA, September 2001.

CONCLUSIONS

Through the Task I research, the results have fully demonstrated the feasibility of the TMD for improving breast examination technique in diagnosis, documentation, and training. In particular, the results have shown that new tactile mapping technology can quantitatively measure the location and applied forces in breast palpation, and the tactile features of detected breast lumps; the prototype interactive training program can track finger motions and applied forces during breast palpation in which the on-line feedback can help the training to better understand the search strategy and adjust applied force level to increase the sensitivity.

In addition to the demonstration of feasibility for planning the Task II project, this research has also enable many further applications for tactile mapping in breast cancer diagnosis and treatment. The tactile lesion characterization effort will contribute to our fundamental understanding of the mechanical interactions in palpation, so that optimal sensors and palpation strategies can be developed. By knowing the advantages and limitations of the sensors and the associated algorithms with respect to the detection capability and accuracy for deeper or smaller lesions, the clinical applications can be better defined.

REFERENCES

1) Feig SA. Screening guidelines and controversies. In Bassett LW, Jackson VP et al. Diagnosis of Diseases of the Breast. pp 329-343. WB Saunders Co, Philadelpia 1997

2) Tabar L, Fagerberg G, Duffy SW, et al. Update of the Swedish two-county program of mammographic screening for breast cancer. Radiologic Clinicsl of NA, 1992. 30: 187-210.

3) Society of Surgical Oncology Practice Guidelines. Breast cancer surgical practice guidelines. Oncology. 1997. 11: 877-886,

4) Rimer BK. Breast Cancer Screening. In Harris JR, Lippman ME, Morrow M, Hellman S. Diseases of the Breast. 1996. Pp 307-322.

5) Geng, J, "Rainbow 3D Camera - A New Concept for High Speed and Low-Cost 3D Vision", *Journal of Optical Engineering* Vol.35, No.2, p376, Feb 1996.

6) Wang Y, Nguyen C, Srikanchana R, Geng J, and Freedman MT, "Tactile mapping of palpable abnormalities for breast cancer diagnosis," *Proc. IEEE Conf. Robotics and Automation*, Detroit, 1999.

7) R. Srikachana, Y. Wang, C. Nguyen, and M. T. Freedman, "Soft Tissue Modeling in Palpable Lesion Characterization by Tactile Mapping Neural Networks," to appear *Proc. Intl. Joint Congress Neural Nets*, 1999.

8) Zeng J, Wang Y, Freedman MT, and Mun SK, "Finger tracking for breast palpation quantification using color image features," *Journal of Optical Engineering*, 36(12): 3455-3461, December 1997.

9) Y. Wang, S-H Lin, H. Li, and S-Y Kung, "Data Mapping by Probabilistic Modular Networks and Information Theoretic Criteria," *IEEE Transactions on Signal Processing*, vol. 46, no.12, pp. 3378-3397, December 1998.

10) Y. Wang and J. M. Morris, "On Numerical Verification of Time-Domain Moment Method in Ultrasound Tomography," *SPIE Journal of Biomedical Optics*, vol. 1, No. 3, pp. 324-329, July 1996.

11) Y. Wang and T. Adali, "Probabilistic neural networks for parameter quantification in medical image analysis," in *Biomedical Engineering Recent Development*, pp.669-672, J. Vossoughi, Editor, 1994.

12) Adames CK, Hall DC, Stein GH, Stephenson HS, Goldstein MK, and Pennypacker HS, "Lump detection in simulated human breasts," *Perception and Psychophysics*, 20(3), pp.163, 1976.

13) Dario, P and Bergamasco, M, "An advanced robot system for automated diagnosis tasks through palpation," *IEEE Trans. Biomed. Eng.*, vol. 35, no. 2, pp.118-126, February 1988.

14) Fearing, RS, "Tactile sensing mechanisms," *Intl. J. Robotics Research*, 9(3): 3-23, 1990.

15) Fletcher SW, O'Malley MS, and Bunce LA, "Physician's abilities to detect lumps in silicone breast models," *JAMA*, 253(15):2224-2228, 1985.

16) Howe, RD, Peine WJ, Kontarinis, DA, Son, J, "Remote palpation technology," *IEEE Engineering in Medicine and Biology*, 14(3): 318-323, May/June 1995.

17) Wellman, PS, "A biomechanical model for tactile mapping of palpable abnormalities," Harvard Robotics Lab Technical Report 96-002, Harvard University, 1996.

18) Gaston MH and Moody LE, "Improving utilization of brest and cervical cancer screening in your office practice," *Journal of National Medical Association*, 87(9): 700-704, 1995.

19) Foster RS, Worden JK, Costanza MC, and Solomon LJ, " Clinical breast examination and breast self-examination: past and present effect on breast cancer survival," *Cancer*, 69(7): 1992-1998, 1992.

20) American Cancer Society Brochure F-362, *How to Examine Your Breasts*, 1994.

21) J. Ophir, I. Cespedes, H. Ponnekanti, Y. Yazdi, and X. Li, "Elastography: a quantitative method for imaging the elasticity of biological tissues," *Ultrasonic Imaging*, 13:111-134, 1991.

22) C. D. Haagensen, *Physicians' Role in the Detection and Diagnosis of Breast Disease: Palpation of the Breast, Diseases of The Breast*, 3rd ed. Philadelphia: Saunders, pp.521-527, 1986.

23) H. S. Bloom et als., "Major stimulus dimensions determining detection of simulated breast lesions," *Perception and Psychophysics*, Vol. 32, pp. 251-260, 1982.

24) D. C. Hall, C. K. Adams, G. H. Stein, H. S. Stephenson, M. K. Goldstein, and H. S. Pennypacker, "Improved Detection of Human Breast Lesions," *Cancer*, Vol. 46, pp. 400-413, July 1980.

25) B. P. Haughey, J. R. Marshall, C. Mettlin, T. Nemoto, K. Kroldart, and M. Swanson, "Nurse's Ability to Detect Nodules in Silicone Breast Models," *Oncology Nursing Forum*, Vol. 11, No. 1, pp. 37-42, 1984.

26) M. S. O'Malley and S. W. Fletcher, "Screening for Breast Cancer With Breast Self-Examination A Critical Review," *JAMA*, Vol. 257, No. 16, pp. 2197-2203, 1987.

27) R. D. Howe, "Touch sensing and display for surgical applications," robotics, Vol. 4, No. 1, 1995.

28) R. D. Howe et als., "A tactile sensing and display system for teleoperated manipulation," *Proc. IEEE Intl. Conf. Robotics Auto.*, pp. 641-646, Nagoya, Japan, May 1995.

29) R. S. Fearing and J. M. Hollerbach, "Basic solid mechanics for tactile sensing," *Intl. J. Robotics Research*, 4(3): 40-54, Fall 1985.

30) J. M. Rehg and T. Kanade, "Visual tracking of high DOF articulated structures: an application to human hand tracking," *Proc. 3th European Conf. Computer Vision*, 1994.

31) E. J. Nicolson, "Tactile sensing and control of a planar manipulator," Ph.D. Thesis, University of California Berkeley, 1994.

32) E. J. Nicolson and R. S. Fearing, "The reliability of curvature estimates from linear elastic tactile sensors," *Proc. IEEE Intl. Conf. Robotics Auto.*, Nagoya, Japan, May 1995.

33) H. Y. Yu and S. C. Sanday, "Elastic field in joined semi-infinite solids with an inclusion," *Proc. R. Sec. Lend.*, A 434:521-530. 1991.

34) R. D. Howe and M. R. Kutkosky, "Dynamic tactile sensing: perception of fine surface features with stress rate sensing," *IEEE Trans. Robotics & Auto.*, 9(2):140-151, April 1993.

35) R. S. Fearing and T. O. Binford, "Using a Cylindrical Tactile Sensor for Determining Curvature," *IEEE Trans. Robotics and Automation,* December 1991.

36) B. Gray and R. S. Fearing, "A Surface-Micromachined Microtactile Sensor Array," *IEEE ICRA*, Minneapolis, April 1996.

37) W. J. Peine and R. D. Howe, "Finger Pad Shape in Lump Detection," *ASME Summer Bioeng. Conf.,* Sun River Oregon, June 1997.

38) A. Sarvazyan, "Knowledge-Based Mechanical Imaging of the Breast," *Medical Technology*, Washington, DC 1997.

39) P. S. Wellman and R. D. Howe, "Modeling Probe and Tissue Interaction for Tumor Feature Extraction," *ASME Summer Bioeng. Conf.,* Sun River Oregon, June 1997.

40) R. T. Senie, *et al.,* "Method of tumor detection influences disease-free survival of women with breast carcinoma," *Cancer*, vol. 73, no. 6, pp. 1666-1672, March 1994

APENDICES

Non-Rigid Image Registration by Neural Computations, R. Srikanchana, K. Woods, J. Xuan, C. Nguyen, and Y. Wang, *Proceedings of IEEE Neural Networks for Signal Processing,* 2001.

Tactile Mapping of Palpable for Breast Cancer Diagnosis, R. Srikanchana, C. Nguyen, and Y. Wang, *VACETS Technical International Conference,* 2001.

NON-RIGID IMAGE REGISTRATION BY NEURAL COMPUTATIONS

Rujirutana Srikanchana   Kelvin Woods   Jianhua Xuan
Charles Nguyen   Yue Wang
Department of Electrical Engineering and Computer Science
The Catholic University of America, Washington, DC 20064, USA

Abstract. This paper describes a neural computation based non-rigid registration methodology using multiple rigid transforms, in a piece-wise fashion, to model the registration process between images in a sequence. The registration methodology is a hybrid approach that combines registration without exact point correspondence via multi-object principal axes, and registration with point correspondence via polynomial transform. Neural computation is used to combine the derived individual principal axes solutions for each object in a committee machine formulation and to obtain the polynomial transform based on extracted control points using a multi layer perceptrons (MLP). Three examples are presented to demonstrate the techniques involved in the process. The first example uses four Gaussian clusters and focuses on the combination of the multiple transforms into a composite transform using finite mixture modeling techniques [14]. The next examples present the complete process for prostate cancer registration and breast sequence analysis respectively. To verify performance, the results are compared to non-neural based implementations and other existing registration methods.

INTRODUCTION

The estimation of transformational geometry from two point sets is an essential step to medical image fusion and computer vision [1, 2]. Medical diagnosis, for instance, often benefits from the complementary of the information in images of different modalities. The task is to recover a matrix representation requiring a set of correspondence matches between features in the two coordinate system [3]. Assume two 3-D data point sets $\{p_{iA}\}$ and $\{p_{iB}\}$; $i = 1, 2, ..., N$ are related by

$$p_{iB} = Rp_{iA} + T + N_i \qquad (1)$$

---

using a single neural network gives the edge degradation by the influence of blockwise processing as shown in Figure 7(b). On the other hand, the proposed compression method gives better reconstructed image compared with a single neural network as shown in Figure 7(c). Moreover, from Figure 7(d), it can be seen that the proposed compression method gives an adequate result for region segmentation. Namely, the blocks with the smallest size are allocated in the edge regions and the blocks with the larger size are allocated in the flat regions.
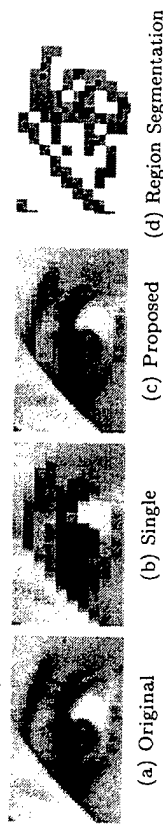
Figure 7: Enlarged images around an eye.

(a) Original   (b) Single   (c) Proposed   (d) Region Segmentation

CONCLUSIONS

This paper has proposed a lossy compression method for gray images on the basis of a modular structured neural network. This modular structured neural network has consisted of multiple neural networks with different block sizes (the numbers of input units) for the region segmentation. By the region segmentation procedure, each neural network has been assigned to each region such as the edge or the flat region. From simulation results it has been shown that the proposed compression method gives better compression performance compared with the conventional compression method using a single neural network. Moreover, the proposed compression method has obtained reasonable results for region segmentation.

REFERENCES

[1] G.W.Cottrell, P.Munro and D.Zipser, "Image Compression by Back Propagation: An example of extensional programming," ICS Report 8702, **Institute for Cognitive Science, University of California, San Diego,** 1987.

[2] R. A. Jacobs, M. I. Jordan and A. G. Barto, "Task Decomposition Through Competition in a Modular Connectionist Architecture: The What and Where Vision Tasks," **Cognitive Science,** vol. 15, pp. 219–250, 1991.

[3] A. Namphol, S. H. Chin and M. Arozullah, "Image Compression with a Hierachical Neural Network," **IEEE Trans. on Aerospace and Electonic Systems,** vol. 32, no. 1, pp. 326–338, 1989.

[4] N. M. Rahim and T. Yahagi, "Image compression by new sub-image block classification techniques using neural networks," **IEICE Trans. on Fundamentals,** vol. E83-A, no. 10, pp. 2040–2043, 2000.

[5] D. E. Rumelhart, J. L. McClelland and the PDP Research Group, **Parallel Distributed Processing,** vol. I, Cambridge, MA: MIT Press, 1986.

where $\mathbf{R}$ is a rotation matrix, $\mathbf{T}$ is a translation vector, and $\mathbf{N}_i$ is a noise vector. Given $\{\mathbf{p}_{iA}\}$ and $\{\mathbf{p}_{iB}\}$, Arun *et. al* present an algorithm for finding the least-squares solution of $\mathbf{R}$ and $\mathbf{T}$, which is based on the decoupling translation and rotation and the singular value decomposition (SVD) of a 3×3 cross-covariance matrix [3].

The major limitation of the present method is twofold: (1) while feature matching methods can give quite accurate solutions, obtaining correct correspondences of features is a hard problem, especially in the cases of images acquired using different modalities or from inter-subjects; and (2) a rigidity assumption is heuristically imposed while those newly developed deformable matching methods can be computationally expensive and typically need good initial guesses to assure correct convergence [2, 4]. One popular method that is correspondenceless is the principal axes registration (PAR) [1], that is based on the relatively stable geometric properties of image features, i.e., the geometric information contained in these stable image features is often sufficient to determine the transformation between images [2]. Once again, it cannot handle the cases with non-rigid objects.

In this paper, we present a neural computation based non-rigid registration using piece-wise rigid transformation. The novel feature is to align two point sets without needing to establish explicit point correspondences, where the derivation is realized by minimizing the relative entropy between the two point distributions resulting in a maximum likelihood estimate of the transformation matrix. A committee machine approach is used for recovering the transformational geometry of the non-rigid structures. That is rather than using a single transformation matrix which gives rise to a large registration error, we attempt to interpolatively apply a mixture of transformations. By further generalizing PAR to a finite mixture registration (FMR) scheme, with a soft partitioning of the data set, the mixture is fit using expectation-maximization (EM) algorithm. We then applied a probabilistic adaptive principal components extraction (PAPEX) algorithm [10], to estimate the transformational of the orthogonal set of eigenvalues and eigenvectors of the auto-covariance matrix. By applying a committee machine to a non-rigid registration, using FMR as the experts and PAPEX as a gating function, we can acquire the registration based on a mixture of piece-wise transformations of the data set. Then the correspondences control points are obtained. As a final step, the warped image is obtaining using the neural network based non-linear mapping, to obtain the polynomial transform based on extracted control points using MLP.

THEORY AND METHOD

Suggested by information theory [5], we note that, since the control point sets in two images can be considered as two separate realizations of the same random source, we do not need to establish point correspondences to extract the transformation matrix. In other words, if we denote by $P_{\{P_i\}}$ the distribution

of the control point set in an image, we have the simple relationship

$$P_{\{P_{iB}\}} = P_{\{R P_{iA} + T\}} + \epsilon \quad (2)$$

where ϵ is the noise component. Since the probability distributions can be computed independently on each image without any need to establish feature correspondences, and given the two distributions of the control point sets in the two images, we can recover the transformation matrix in a simple fashion [2], as we now sketch.

For observation of the distributions, we can estimate $\mathbf{R}$ and $\mathbf{T}$ by minimizing the relative entropy (Kullback-Leibler distance) between $P_{\{P_{iB}\}}$ and $P_{\{R P_{iA}+T\}}$. The least relative entropy estimator is then defined as

$$\arg\min_{\mathbf{R},\mathbf{T}} D(P_{\{P_{iB}\}} \| P_{\{R P_{iA}+T\}}) \quad (3)$$

where D denotes the relative entropy measure. Following the same strategy to decoupling translation and rotation as in [3], we can define a new data point by $\mathbf{q}_{iA} = \mathbf{p}_{iA} - \mathbf{p}_A^0$ and $\mathbf{q}_{iB} = \mathbf{p}_{jB} - \mathbf{p}_B^0$, where $\mathbf{p}_A^0$ and $\mathbf{p}_B^0$ are the centroids of $\{\mathbf{p}_{iA}\}$ and $\{\mathbf{p}_{jB}\}$ respectively. Then the optimal geometric transformations, $\mathbf{R}$ and $\mathbf{T}$, are defined as

$$\mathbf{R} = \mathbf{U}_B \mathbf{H} \mathbf{U}_A^t \quad \text{and} \quad \mathbf{T} = \mathbf{p}_B^0 - \mathbf{R} \mathbf{p}_A^0 \quad (4)$$

where the superscript t denotes matrix transposition, $\mathbf{U}_A$ and $\mathbf{U}_B$ are 3×3 orthonormal matrices, and $\mathbf{H}$ is a 3×3 diagonal matrix with element $h_m = \sqrt{\lambda_{mB}/\lambda_{mA}}$. Note that the transformation $\mathbf{U}$ consists of the orthonormal set of eigenvectors and h_m is the squared root of the eigenvalues λ_m of the auto-covariance matrix $\mathbf{C}$ for $m = 1, 2, 3$ and for $\{\mathbf{p}_{iA}\}$ and $\{\mathbf{p}_{jB}\}$, respectively.

However, because of its global linearity, the application of PAR is necessarily somewhat limited [6]. An alternative paradigm is to model a multimodal control point set with a collection of local linear models. The method is a two-stage procedure: a soft partitioning of the data set followed by estimation of the principal axes within each partition [7]. Recently there has been considerable success in using standard finite normal mixture (SFNM) to model the distribution of a multimodal data set and the association of a SFNM distribution with PAR offers the possibility of being able to register two images through a mixture of probabilistic principal axes transformations [7]. Assume that there are K_0 control point clusters, where each control point cluster defines a transformation $\{\mathbf{R}_k, \mathbf{T}_k\}$. Thus for a point $\mathbf{p}_{nA}$, its new locations corresponding to each of the transformations are $\mathbf{p}_{nk} = \mathbf{R}_k \mathbf{p}_{nA} + \mathbf{T}_k$ for $k = 1,...,K_0$. Further assume that the control point set defines a SFNM distribution

$$f(\mathbf{p}_i) = \sum_{k=1}^{K_0} \pi_k g(\mathbf{p}_i | \boldsymbol{\mu}_k, \mathbf{C}_k) \quad (5)$$

where g is the Gaussian kernel with mean vector $\boldsymbol{\mu}_k$ and auto-covariance matrix $\mathbf{C}_k$, and π_k is the mixing factor proportional to the number of control

points in cluster k. For each of the control point sets $\{p_{iA}\}$ and $\{p_{iB}\}$, the mixture is fit using the expectation-maximization (EM) algorithm. The E step involves assigning to the linear models responsibilities from the control points; the M step involves re-estimating the parameters of the linear models in the light of this assignment [7].

Thus the statistical membership of point p_{nA} belonging to each of the control point clusters can be derived by

$$z_{nk} = P(R_k, T_k | p_{nA}) = \frac{\pi_{kA} g(p_{nA} | \mu_{kA}, C_{kA})}{f(p_{nA})} \quad (6)$$

i.e., the posterior probability of $\{R_k, T_k\}$ given p_{nA}. Thus, we can define the FMR transformation as

$$p_n = \sum_{k=1}^{K_0} z_{nk} p_{nk} = \sum_{k=1}^{K_0} \frac{\pi_{kA} g(p_{nA} | \mu_{kA}, C_{kA})}{f(p_{nA})} (R_k p_{nA} + T_k) \quad (7)$$

where $\{R_k, T_k\}$ is determined based on $f(p_i) = \sum_{k=1}^{K_0} \pi_k g(p_i | \mu_k, C_k)$ that we have estimated in the previous step using the EM algorithm. Note that now we do not need the correspondences between the two control point clusters, and these correspondences may be found, after a global PAR is initially performed, by using a site model supported approach or a dual-step EM algorithm to unify the tasks of estimating transformation geometry and identifying cluster-correspondence matches [4]. This philosophy for recovering transformational geometry of the non-rigid objects is similar in spirit to the *divide-and-conquer* principle [6], under which the relative entropy between the two point sets reaches its minimum

$$\arg \min_{R_k, T_k} D(P_{\{p_{iB}\}} \| P_{\{\sum_{k=1}^{K_0} z_{ik}(R_k p_{iA} + T_k)\}}) \quad (8)$$

both globally and locally.

Based on a mixture of probabilistic principal axes transformations, the next section describes a neural computation using a committee machine approach for which a complex computational task is solved by dividing it into a number of computationally simple tasks and then combining the solutions to those tasks. Basically, it fuses knowledge acquired by experts to arrive at an overall decision that is supposedly superior to that attainable by any one of them acting alone.

NEURAL COMPUTATION

A neural network interpretation of the EM algorithm is given in [8]. Because of its reputation of being slow in which new information acquired in the expectation step is not used immediately, on-line versions of the EM algorithm are proposed for large-scale sequential learning. Thus, we adopt a fully unsupervised and incremental stochastic learning algorithm. The

scheme provides winner-takes-in probability (Bayesian "soft") splits of the control points, hence allowing the data to contribute simultaneously to multiple clusters which results in

$E - Step$

$$z_{(i+1)k} = \frac{\pi_k^{(i)} g(p_{i+1} | \mu_k^{(i)}, C_k^{(i)})}{f(p_{i+1} | \pi_k^{(i)}, \mu_k^{(i)}, C_k^{(i)})} \quad (9)$$

$M - Step$

$$\mu_k^{(i+1)} = \mu_k^{(i)} + a(i)(p_{i+1} - \mu_k^{(i)}) z_{(i+1)k}, \quad (10)$$

$$C_k^{(i+1)} = C_k^{(i)} + b(i)[(p_{i+1} - \mu_k^{(i)})(p_{i+1} - \mu_k^{(i)})^T - C_k^{(i)}] z_{(i+1)k}, \quad (11)$$

$$\pi_k^{(i+1)} = \frac{i}{i+1} \pi_k^{(i)} + \frac{1}{i+1} z_{(i+1)k} \quad (12)$$

for $k = 1, ..., K_0$ and for $\{p_{iA}\}$ and $\{p_{iB}\}$, respectively, where $a(i)$ and $b(i)$ are introduced as the learning rates, two sequences converging to zero, ensuring unbiased estimates after convergence. This procedure is termed as neural computation of the EM algorithm, where at each complete cycle of the algorithm, we first use "old" set of parameter values to determine the posterior probabilities $z_{(i+1)k}$. These posterior probabilities are then used to obtain "new" values $\pi_k^{(i+1)}, \mu_k^{(i+1)}, C_k^{(i+1)}$. The algorithm cycles back and forth until the value of relative entropy between the data histogram and mixture model reaches its minimum

$$\arg \min_{\pi_k, \mu_k, C_k} D(P_{\{p_i\}} \| f(p_i)) \quad (13)$$

for $\{p_{iA}\}$ and $\{p_{iB}\}$, respectively.

With a soft partitioning of the data set using Eqs. (9-12), control points will now effectively belong to more than one cluster spatially. Thus, the effective input values are $p_{ik} = z_{ik}(p_i - \mu_k)$ for an independent registration transformation k in the committee machine [9]. We then extend our adaptive principal components extraction (APEX) algorithm to a probabilistic version, i.e., PAPEX [10], to determine U_k for $\{p_{iA}\}$ and $\{p_{iB}\}$, respectively, summarized as follows.

1. Initialize the feedforward weight vector u_{mk} for $m = 1, 2, 3$, and the feedback weight vector a_{mk} to small random values for $m = 2, 3$, at time $i = 1$. Assign a small positive value to the learning rate parameter η.

2. Set $m = 1$, and for $i = 1, 2, ...$, compute

$$y_{1k}(i) = u_{1k}^T(i) z_{ik}(p_i - \mu_k) \quad (14)$$

$$u_{1k}(i+1) = u_{1k}(i) + \eta[y_{1k}(i) z_{ik}(p_i - \mu_k) - y_{1k}^2(i) u_{1k}(i)] \quad (15)$$

For large i we have $u_{1k}(i) \longrightarrow u_{1k}$, where u_{1k} is the eigenvector associated with the largest eigenvalue of the cluster k, and $\lambda_{1k} = \frac{1}{N} \sum_{i=1}^{N} y_{1k}^2(i)$.

Figure 1: A mixture Gaussian data set (left: Gaussian model; middle: FMR registration result; right: inverse FMR result)

RESULTS AND DISCUSSIONS

To evaluate the effectiveness of our algorithm, three simulations were performed. The first simulation explored the performance of FMR under controlled conditions while the other two simulations considered the complete processing chain applied to real world problems. Next, each of these simulations is discussed.

The first simulation is a mixture of 600 data points generated from four Gaussian clusters in 3-D space. Figure 1(left) is the original image; the global view of the data clearly suggests the presence of four distinct clusters within the data. We considered three of the four Gaussian clusters as the control objects and the remaining object as a noncontrol object. Each of the clusters were translated and rotated by different amounts to simulate a non-global transform. With a mixture of all the three local transforms, we acquired a non-rigid transform of a non-control object based on a committee machine approach as shown in Figure 1(middle). To show the robustness of our propose method, we applied our algorithm to the transformed image as an inverse process resulting in Figure 1(right). The performance metric is mean square error (MSE) of the non-control object. Several runs of this example were conducted to average out randomness of the data points. The results show a MSE of 7.6% between the final image and original. Thus, showing the usefulness of this approach.

Next, we extended our algorithm to a 3-D prostate registration problem. Based on our previous work [14], this 3-D model contains a precise probabilistic map of prostate tumor distribution and the corresponding anatomic structure of a prostate. The goal of this example is to register the tumor inside a prostate, with a reference model using prostate anatomic structure as a control objects. We denote the reference model as shown in Figure 2(left) and the float model with non-control object as shown in Figure 2(middle). We find object to object corresponding and let tumor in the float model be a non-control object. After we applied our hybrid committee machine algorithm to the reference and the float model, based on piece-wise registration, each control points are effectively belong to more than one cluster hence allowing the data to contribute simultaneously to multiple clusters. Figure 2(right) shows the result using neural computation to register tumor in a float model to a reference model.

---

3. Set $m = 2$, and for $i = 1, 2, \ldots$, compute

$$\mathbf{y}_{(m-1)k}(i) = [y_{1k}(i), y_{2k}(i), \ldots, y_{(m-1)k}(i)]^T \quad (16)$$

$$y_{mk}(i) = \mathbf{u}_{mk}^T(i)z_{ik}(\mathbf{p}_i - \boldsymbol{\mu}_k) + \mathbf{a}_{mk}^T(i)\mathbf{y}_{(m-1)k}(i) \quad (17)$$

$$\mathbf{u}_{mk}(i+1) = \mathbf{u}_{mk}(i) + \eta[y_{mk}(i)z_{ik}(\mathbf{p}_i - \boldsymbol{\mu}_k) - y_{mk}^2(i)\mathbf{u}_{mk}(i)] \quad (18)$$

$$\mathbf{a}_{mk}(i+1) = \mathbf{a}_{mk}(i) - \eta[y_{mk}(i)\mathbf{y}_{(m-1)k}(i) + y_{mk}^2(i)\mathbf{a}_{mk}(i)] \quad (19)$$

For large i we have $\mathbf{u}_{2k}(i) \longrightarrow \mathbf{u}_{2k}$, where $\mathbf{u}_{2k}$ is the eigenvector associated with the second largest eigenvalue of the cluster k, and $\lambda_{2k} = \frac{1}{N}\sum_{i=1}^N y_{2k}^2(i)$.

4. Set $m = 3$, go to step 3. For large i we have $\mathbf{u}_{3k}(i) \longrightarrow \mathbf{u}_{3k}$, where $\mathbf{u}_{3k}$ is the eigenvector associated with the third largest eigenvalue of the cluster k, and $\lambda_{3k} = \frac{1}{N}\sum_{i=1}^N y_{3k}^2(i)$.

The neural computational of a committee machine can be achieved by distributing the learning tasks among a number of experts, which in turn partitioning the input space into a set of subspaces. The experts are in theory performing supervised learning in that there individual outputs are combined to model the desired response. There is, however, a sense in which the experts are also performing self-organized learning; that is, they self organize to find a good partitioning of the input space so that each expert does well at modeling its own subspace, and as a whole group they model the input space well.

Consider the modular network nature of Eq. (7), it is a mixture of local expert model, in which the individual responses of the experts are nonlinearly combined by means of a single gating network. It is assume here that the different experts work best in different regions of the input space in accordance with the probabilistic generative model. In our case, the effective input values are $\mathbf{p}_{ik} = z_{ik}(\mathbf{p}_i - \boldsymbol{\mu}_k)$ for an independent registration transformation k in the networks. A committee machine consists of k supervised modules, with a soft partitioning of the data set using EM algorithm called experts, and an integrating unit called a gating network that performs the function PAPEX to determine the transformation of the orthogonal set of eigenvalues and eigenvectors of the auto-covariance matrix among the expert networks. The output of our committee machine is a transformational matrix of image pair. Based on those correspondences between the two images, the control points are obtained. The final step is to calculate the polynomial transformation using piece-wise interpolation. In our case for a given corresponding control points pair of the image, we considered neural network based MLP to acquired the polynomial transform. The final result shows the warped image that has been corrected by applied our neural computation to correct most of the scale different between the images.
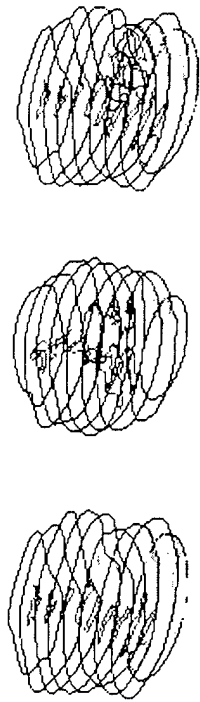
Figure 2: Prostate Model used in registration (left: reference model; middle: float image; right: registration cancer class of float image to reference image using FMR method)

As a final example, we applied our algorithm to a temporal sequence of mammograms of a single patient [15]. In this example, the committee machine is used to obtain an initial registration using multiple extracted objects (skinline, dense tissue regions) in a finite mixture scheme. Then MLP was used to determine the coefficients of a polynomial transform using extracted vertical and horizontal cross points of elongated structures as control points. Previously, thin-plate spline (TPS) was used to determine the transform coefficients [13]. As a comparison, we consider both results here. Figure 3 shows the raw sequence and Figure 4 shows the resulting warped image for MLP (left) and TPS (right). From visual inspection we see that by using MLP the most of the scale different between images has been corrected. While the TPS distorts the image, this distortion can be attributed to control point selection and correspondence. The MLP better adapts to the error present in the control points thus yielding a smoother result.

CONCLUSION

In this paper, we presented the theoretical concepts and methods of a neural computation based non-rigid registration algorithm. The approach uses
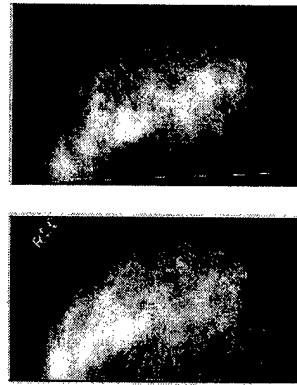

Figure 3: A pair of real mammograms taken over a period of time from the same patient.
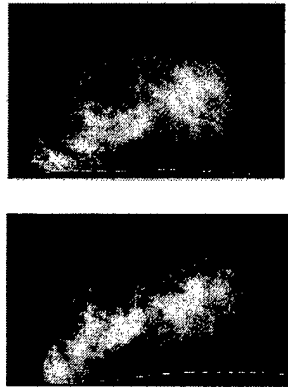

Figure 4: The result of warped current image to previous image (left: MLP; right: TPS).

a committee machine to recover the total transformational geometry of the non-rigid object using multiple rigid transforms combined together in a finite mixture registration scheme. Finite mixture transform combination is a novel technique to combine multiple transforms that are contained in a single image. Other than local transforms no other method combines multiple transforms together. In addition finite mixture combinations, yields a lower MSE than the local transform and results in a smooth image while local transforms yield an image containing discontinues on transform boundaries. In addition, the registration obtained in the committee machine is fine tuned using a non-linear transform generated by a MLP network using extracted control points.

We applied this algorithm to prostrate and breast registration problems with reasonable results as shown in the previous figures. Some distortion can be seen in the final warped images because of the error in control point selection and correspondence. Improvement is this portion should decrease distortion and yield a smoother looking image. Using neural networks in this problem has increased the generality of this approach by allowing the algorithm to adjust performance as imaging condition change.

ACKNOWLEDGMENTS

REFERENCES

[1] M. Moshfeghi and H. Rusinek, "Three-dimensional registration of multimodality medical images using the principal axes techniques," *Phlips J. Res.*, vol. 47, no.2, pp. 81-97, 1992.

MINIMIZING BER IN DFE's WITH THE ADATRON ALGORITHM

Ignacio Santamaría, Carlos Pantaleón

DICOM, ETSII y Telecom, Univ. of Cantabria, Spain

E-mail: nacho,carlos@gtas.dicom.unican.es

Jose C. Principe

Computational NeuroEngineering Laboratory, Univ. of Florida

E-mail: principe@cnel.ufl.edu

Abstract. In this paper we apply the Structural Risk Minimization (SRM) principle to minimize the Bit Error Rate in Decision Feedback Equalizers (DFE). We consider both linear discriminant (Optimal Hyperplane) and nonlinear discriminant (Support Vector Machine) classifiers as an alternative to the linear MMSE-DFE and Radial Basis Function (RBF) networks, respectively. A fast and simple adaptive algorithm called the Adatron is applied to obtain the linear or nonlinear classifier. In this way we avoid the high computational cost of quadratic programming. We also study the performance of soft margin classifiers: it is shown that to consider a regularized problem improves the BER, mainly at low SNR's. Furthermore, an adaptive implementation is discussed. Some simulation examples show the advantages of the proposed linear (OH) and nonlinear (SVM) DFE's: a better performance in comparison to the linear MMSE-DFE and a simpler structure in comparison to the RBF-DFE.

INTRODUCTION

In many digital communication receivers, a DFE is used to compensate the intersymbol interference (ISI) caused by the channel. In the equalizer literature, both a linear filter and the RBF network are being proposed for the feedforward filter in DFE's [1, 2, 3]. The RBF network can approach the optimal Bayesian detector [3], while the conventional FIR can be thought as a linear regressor in the input/ desired response space. Therefore, they implement respectively a nonlinear and linear discriminant function, and they both utilize the Minimum Mean Square Error (MMSE) criterion in choosing the optimal weights.

However, it is well known that, in general, the MMSE design does not

[2] V. Govindu and C. Shekhar, "Alignment using distributions of local geometric properties," *IEEE Trans. Pattern Anal. Machine Intell.*, vol. 21, no.10, pp. 1031-1043, October 1999.

[3] K. S. Arun, T. S. Huang, and S. D. Blostein, "Least-Squares Fitting of Two 3-D Point Sets," *IEEE Trans. Pattern Anal. Machine Intell.*, vol. 9, no.5, pp. 698-700, September 1987.

[4] A. D.J. Cross and E. R. Hancock, "Graph matching with a dual-step EM algorithm," *IEEE Trans. Pattern Anal. Machine Intell.*, vol. 20, no.11, pp. 1236-1253, November 1998.

[5] T. M. Cover and J. A. Thomas, *Elements of Information Theory*, New York: Wiley, 1991.

[6] G. E. Hinton, P. Dayan, and M. Revow, "Modeling the manifolds of images of handwritten digits," *IEEE Trans. Neural Nets*, vol. 8, no.1, pp. 65-74, January 1997.

[7] Y. Wang, L. Luo, M. T. Freedman, and S. Y. Kung, "Probabilistic principal component subspaces: A hierarchical finite mixture model for data visualization," *IEEE Trans. Neural Nets*, vol. 11, no. 3, pp. 625-636, May 2000.

[8] L. Perlovsky and M. McManus, "Maximum likelihood neural networks for sensor fusion and adaptive classification," *Neural Networks*, vol. 4, pp. 89-102, 1991.

[9] S. Haykin, *Neural Networks: A Comprehensive Foundation*, 2nd ed., Prentice-Hall, Inc., Upper Saddle River, Ney Jersey, 1999.

[10] S. Y. Kung, *Principal Component Neural Networks*, New York: Wiley, 1996.

[11] M. I. Jordan and R. A. Jacobs, "Hierarchical mixture of experts and the EM algorithm," *Neural Computation*, vol. 6, pp. 181-214, 1994.

[12] D. M. Titterington, A. F. M. Smith, and U. E. Markov, *Statistical analysis of finite mixture distributions*. New York: John Wiley, 1985.

[13] K. Woods, et. al., "Patient Site Model Supported Change Detection," *Proceedings of SPIE Medical Imaging: 2000*, vol.1, no. 24 , pp. 1095-1106, 2000.

[14] J. Lu, R. Srikanchana, M. McClain, Y. Wang, J. Xuan, I. A. Sesterhenn, M. T. Freedman, and S. K. Mun "A Statistical Volumetric Model for Characterization and Visualization of Prostate Cancer," *Proc. SPIE Medical Imaging*, vol. 3976, pp. 142-153, 2000.

[15] K. Woods, *Image Guided Diagnosis through Change Detection in Image Sequences*, Doctoral Dissertation, The Catholic University of America, 2000.

TACTILE MAPPING OF PALPABLE FOR BREAST CANCER DIAGNOSIS

Rujirutana Srikanchana, Charles C. Nguyen, and Yue Wang

Department of Electrical Engineering and Computer Science
The Catholic University of America
Washington, DC

Abstract: *This paper presents the development of a prototype Tactile Mapping Device (TMD) system comprised mainly of a tactile sensor array probe (TSAP), a 3D camera and a force/torque sensor, which can provide the means to produce tactile maps of the breast lumps during a breast palpation. Focusing on the key tactile topology features from breast palpation such as spatial location, size and shape of the detected lesion, and the force levels used to demonstrate the palpable abnormalities, these maps can record the results of clinical breast examination with a set of pressure distribution profiles and force sensor measurements due to detected lesion. By combining the knowledge of vision based, neural networks and tactile sensing technology are integrated for the investigation of soft tissue interaction with tactile/force sensor, where the hard inclusion (breast cancer) can be characterized through neural network learning capability, instead of using simplified complex biomechanics model with many heuristic assumptions. These maps will serve as an objective documentation of palpable lesions for future comparative examinations. Preliminary results of simulated experiments and limited pre-clinical evaluations of the TMD prototype have pilot-tested our hypothesis and provided solid promising data showing the feasibility of the TMD in real clinical applications.*

1. Introduction

Physical breast examination is an effective and completely non-invasive method for the detection of breast cancer [1-2]. With a lump as the most common symptom of breast cancer, studies show that the majority of breast cancers was found by palpation which complements mammography, since palpation can evaluate breast tissue near the chest wall and axilia that is not accessible to mammography [2]. In addition, studies have found that as many as 12-15% of cancers that were detected by physical examination were not apparent on mammograms [1-2].

Unfortunately, breast palpation has been hampered by problems inherent in its subjective nature, leading to difficulty in interpreting and documenting the examiner's impressions of the perceived lump in terms of tumor characteristics [2]. For example, a physician may determine that a palpable suspicious abnormality needs continued monitoring. This requires maintaining a record of the examination results, which at present is limited to verbal notes about parameters such as the position, size, and hardness of the lump. Because it is difficult to verbalize tactile sensations, the subjective and arbitrary nature of these notes makes effective follow-up exams problematic.

We have conducted a study to advance fundamental understanding of palpation and solve these practical problems through the creation of a new *tactile mapping device* (TMD). This device will measure three key variables during palpation: the examiner's

search patterns, the applied forces, and the small-scale pressure variations at the skin due to lumps. We have integrated and pilot-tested a prototype TMD consisting of a novel three-dimensional (3-D) camera that can track finger motion and breast deformation in video speed, a six degree-of-freedom (DOF) force/torque sensing device measuring the applied forces, and a novel pressure distribution sensor array that can image tactile profile of lumps [1]. The primary objective aims that (1) new tactile mapping technology can quantitatively measure the location and applied forces in breast palpation, and the tactile features of detected breast lumps; and (2) new device can accurately characterize and document breast lumps and will improve clinicians' ability to monitor changes in lump across time and possibly to distinguish malignant from benign lumps. From a set of "images" of the suspect mass, a neural network supported pattern analysis system will extract the invariant properties of the lump, such as the depth and size, based on a nonlinear model of sensor-tissue interaction with hard inclusions. This TMD system will make it possible for the first time to quantitatively and objectively record and characterize the processes and findings of breast palpation. While initially the system will be used to perform clinical breast examination, we believe that eventually it may be used in breast self-examination by women through tele-home care [3-4].

2. System Overview

The goal of this research is to extend the range and resolution of breast palpation methods, thus increasing palpation sensitivity and specificity (i.e, the ability to detect lumps and distinguish clinically significant changes). Using 3-D camera, force sensor, and tactile arrays, we can create reproducible tactile maps of the palpable abnormalities of the breast. The novel 3-D camera invented by the Genex Technologies, Inc. is able to provide real-time 3-D motion measurement (for tactile probe) and surface profile measurement (for breast tissue deformation) at a rate of 30 frames per second. We have further integrated and evaluated related state-of-the-art sensing technologies including tactile sensor array and six DOF force/torque sensor to extract tactile information from breast palpation, where the sensor-tissue interaction of detected palpable lesion can be quantitatively measured and displayed in terms of tactile images. Our laboratory experiments aimed at characterizing the simulated tumors in breast phantom have demonstrated that palpable inclusions can be located to within 1 mm, and the experiment is undergoing for pre-clinical evaluation with real breast tissues.

Our prototype system incorporates a 3-D Rainbow camera, a tactile sensor array probe (TSAP), a breast model with simulated lumps, a force/torque sensor on which the breast model is mounted, and a graphical user interface (GUI). Figure 1 shows a block diagram of the tactile mapping device system to be used for measurement of palpable abnormalities in the laboratory and later in pre-clinical trial. In a typical task, upon detecting a suspicious lump, the examiner will bring the TSAP into contact with the tissue at the palpation site. For a thorough tactile mapping procedure, this involves 3-D positioning the probe through the camera facing the site. The resulting pressure distribution across the probe surface is measured by a Tactile Sensor Array Probe (TSAP) with associated readout electronics. Multiple tactile images with various force levels and torque angles will be required for the lesion characterization. A computer processes the signals to generate appropriate output for visual display on

a monitor or raw data to the physician's office through a telecommunication channel. Below, we describe the components of the tactile mapping system.

2.1 3-D Rainbow Camera

For the accurate positioning of the TSAP, a novel 3-D rainbow camera is adopted in our system, which is suitable for this high-speed 3-D machine vision application. Figure 2 shows the rainbow camera and the acquired sample range image. It exploits a color light projector to illuminate the object in the scene and using an off-the-shelve color camera to obtain a full-frame color image of the scene. The color of the projecting light with spatially continuously varying wavelength is encoded with information of the corresponding projection angle. Each pixel of the color image is associated with a unique ray through the focal point of the camera. Since the angle between camera axis and the ray is known the resulting angle-side-angle triangulation problem can be easily solved when the distance between the light projector and the camera is fixed. Thus, using only one camera, the full frames of 3-D range images can be obtained directly at the camera frame rate (60 frames/s). The spatially varying wavelength light is generated by a white light passing through a linear variable wavelength filter. We have performed experiments to investigate the actual range accuracy and the major error contributors. The results show that the 3-D profile of test artifacts were less than 1 mm. The spatial resolution of the system is limited only by the spatial resolution of the camera optical sensing element and is currently able to provide at least 1024x1024 pixel resolution. When a palpation site is determined, several 3-D range images will be acquired to record the site information.
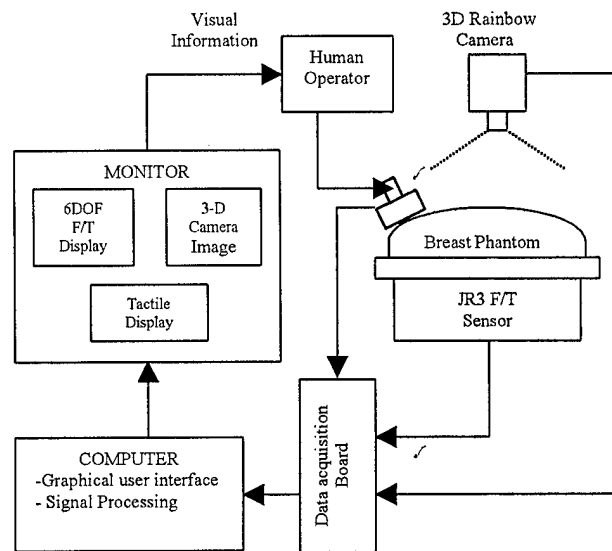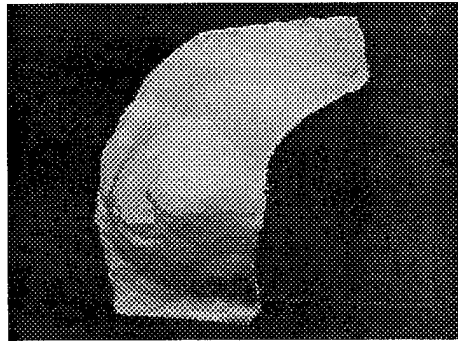
Figure 1. System block diagram.

Figure 2. Three-dimensional range image of the breast model by the Rainbow camera.

2.2 Tactile Sensor Array Probe (TSAP)

Figure 3 illustrates the operation of the capacitive tactile array sensor used in this system. It shows a drawing of the array with the copper layers and the silicone rubber spacers, which is based on the state-of-the-art design by Fearing [5] and Howe [3].

The array is composed of two crossed layers of copper strips separated by thin strips of silicone rubber [5]. Each crossing area forms a capacitor, and when a force is applied onto where the strips cross, the distance between the strips decreases and the capacitance increases [6]. Specially designed electronics will measure the capacitance of each element and relate the capacitance change to the force applied to each element. By measuring the capacitance variations from all the elements simultaneously, we can determine the spatial distribution of pressure across the sensor array. Figure 4 shows a photograph of a commercial prototype TSAP. The sensor array is made with an inexpensive photolithography and etching process and can be easily attached to a variety of probe shapes. In this prototype specification, it is composed of an eight by eight tactile sensor with elements that are 4 mm on a side. The sensor is mounted on a plastic brass backing plate with a surface that has been machined into a section of a square. The backing plate is 5.08 cm on a side and the effective sensing area is 3.20 cm on a side. We decided to make the sensor flat in order to minimize inhomogeneity because the resulting pressure distribution should have a uniform overall signal to noise ratio. The tactile images will then be consistent when used for various breast/chest background textures. The spatial resolution of the tactile array is 4 mm long where the smallest masses that we are currently interested to characterize are on the order of 1 cm in diameter. Smaller elements would increase spatial resolution at the cost of lower coverage area and low sensitivity since the capacitance is proportional to the element area [6]. The tactile sensor has been shielded to provide electronic insulation.
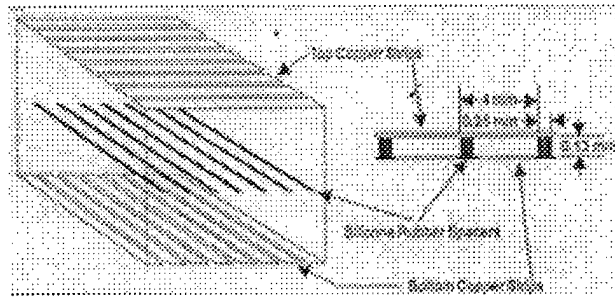
Figure 3. A drawing of a tactile array sensing (adapted from Son 1996).

2.3 Force/Torque Sensing System

The TMD operation requires that the forces/torques exerted by the operator of the TSAP on the breast model be acquired. It would be ideal if a force/torque sensor were to be mounted between the wrist and the hand of the operator. Since it is problematic and impractical to mount a force/torque sensor in such a configuration, we decided to mount it under a base which the breast model is placed on. The forces/torques acquired by the sensor in this configuration can be transformed to those exerted by the operator via proper coordinate transformation. Figure 5 shows a breast model laying on a round base under which a JR^3 force/torque is mounted. The JR^3 force/torque mainly consists of a JR^3 monolithic six DOF force sensor and a JR^3 Intelligent Support System, Comprised of boards for signal conditioning, data acquisition and processing. A computer program was written in Visual C^{++} to request the JR^3 force/torque sensing system to send to the computer six forces/torques along about the Cartesian x-, y-, z-axes assigned to the base. The transmitting and receiving of data between the computer and the force/torque system is carried out through serial port.
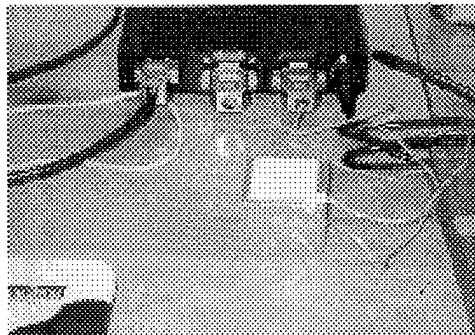

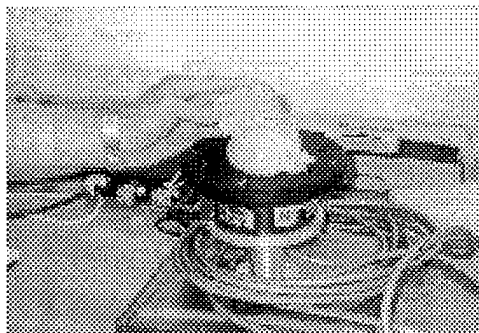Figure 4. A commercial prototype tactile array sensor probe.

Figure 5. JR^3 Force/Torque Sensor

2.4 Breast Models

The breast models used in our laboratory experiments were provided by the HEALTH EDCO, a Division of WRS Group, Inc. The models were made from BIOLIKE^{TM} synthetic tissue that feels just like a real breast [1]. Two models were used in our tests to collect preliminary data. Each of them has 5 lumps that simulate easy- and hard-to-find breast tumors with various sizes and depths at different locations. One of the models is the geriatric breast that is ideally shaped to address the special problems of older women. The geriatric model simulates the natural stretching of the tissue with age. Figure 6 show the distribution of simulated lumps (lesions) in the breast model and the historical spatial distribution of the breast cancer respectively. It should be noticed that as high as 50% of breast cancers occur at the axilia area which is difficult to imaging.
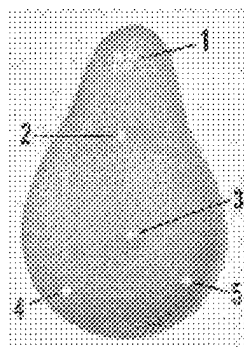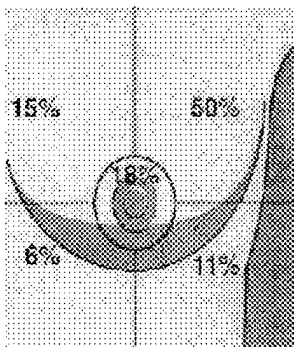

(6.a)   (6.b)

Figure 6.   Breast model with simulated lumps (lesions) (6.a) and the spatial distribution of the locations of breast cancer occurrence (6.b).

2.5 Graphical User Interface

Microsoft Visual C^{++} was employed to implement the GUI to visually display pertinent data of the TSAP and the force/torque sensor. Figure 7a shows the pressure distribution acquired by the TSAP and Figure 7b the time response of the six force/torques applied by the operator.
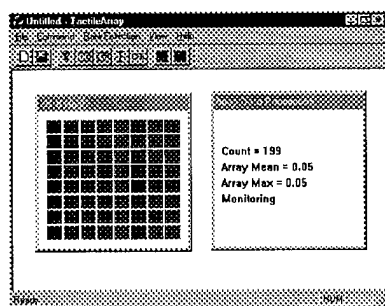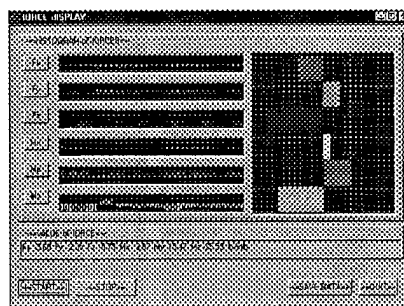
(7.a)   (7.b)

Figure 7. Pressure distribution provided by the TSAP (7.a) and Time response display of forces and torques (7.b).

3. Experimental Results

In order to demonstrate the effectiveness of the TMD system for the characterization and documentation of detected lumps, intensive experiments have been conducted to pilot-test the sensitivity and reproducibility of the system in measuring the applied forces and pressure profiles due to lumps. The primary objective here is to quantitatively acquire tactile measurements of the perceived lesions using the TMD system and to evaluate the performance of the system.

During the experiments conducted below, the forces/torques applied by the human examiner during the palpation are recorded in terms of six force parameter values, i.e., Fx, Fy, Fz, Mx, My, Mz. For the tactile imaging of simulated lesions, the TSAP is used to acquire various tactile images by palpating the site after the examiner locates the lesion by initial hand palpation. Since the relationships between the tactile images and lesion characteristics are expected to be complex and nonlinear, we believe that the inverse problem (extraction of lesion characteristics from tactile images) can be solved when sufficient tactile information is acquired. As a result, for each of the lesions, after pushing the TSAP against the breast to achieve certain level of force, the examiner rotates the TSAP to five different orientations at each of which the information about the forces/torques and tactile image are simultaneously recorded. OR1 is the initial orientation of the TSAP after being pushed by the examiner to certain level of force. OR2, OR3, OR4 and OR5 are the TSAP orientations after it is rotated forward, backward, left and right, respectively.

We carry out the above procedure on two different lesions: Lesion 1 and Lesion 4 as identified in Figure 6.a. Figure 9 shows the 3D mesh surface (Figure 9.a) and the shading interpolation (Figure 9.b) of the pressure distribution measured by the TSAP

for Lesion 1, with the top row for OR1 and the following rows for OR2, OR3, OR4 and OR5. Figure 10 shows the results obtained for Lesion 4 presented in the same manner as Figure 9.
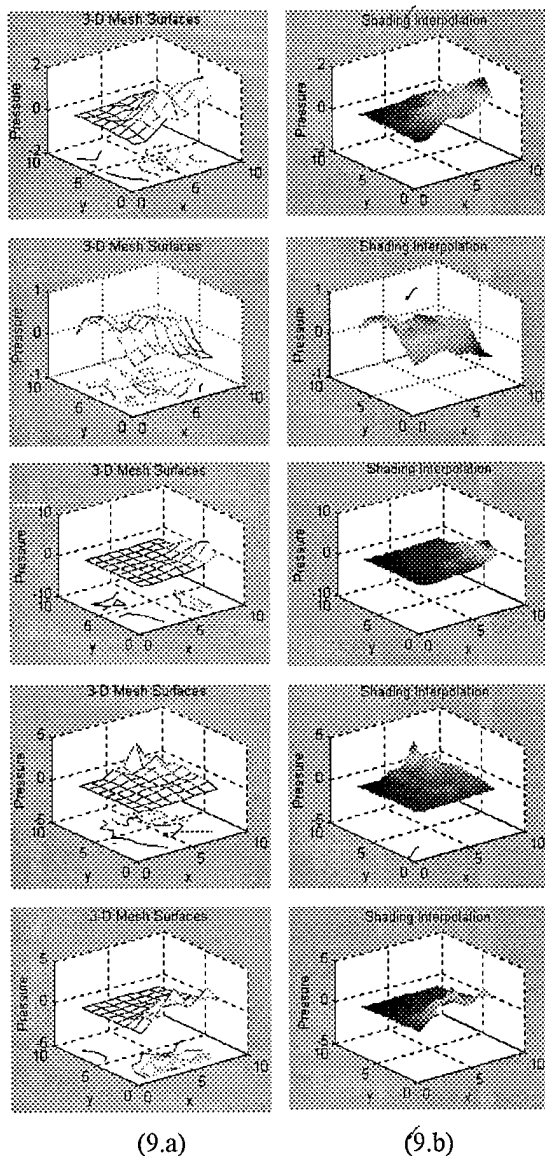

(9.a)   (9.b)

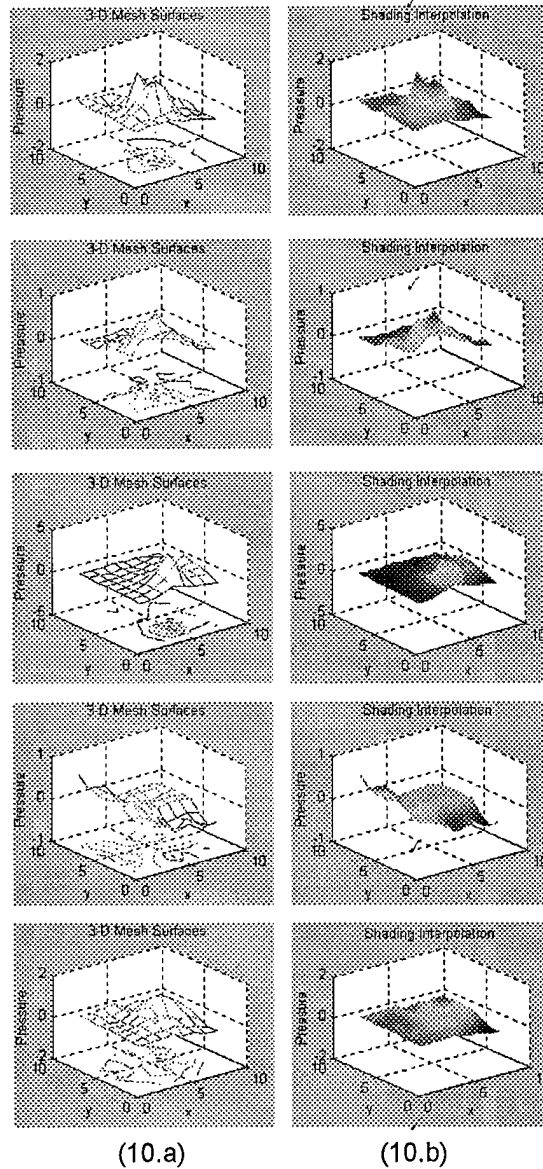Figure 9. Display of experimental results for Lesion 1.

(10.a)   (10.b)

Figure 10. Display of experimental results for Lesion 4.

The values of forces/torques for the experiments conducted for Lesions 1 and 4 are tabulated in Table 1.

Lesion	TSAP Orientation	6DOF Force & Torque (lb/inlb)					
		Fx	Fy	Fz	Mx	My	Mz
1	OR1	-0.89	0.44	-0.13	-2.58	-10.80	0.50
	OR2	-2.34	2.50	-0.10	-5.26	-22.02	1.59
	OR3	1.69	2.96	-0.03	-2.28	-10.50	3.57
	OR4	3.20	-0.38	0.27	0.40	0.40	2.09
	OR5	-1.83	0.38	-0.03	-2.38	-9.32	1.99
4	OR1	-3.17	1.77	-0.16	5.85	25.59	-0.89
	OR2	-2.08	2.48	-0.22	4.37	18.35	1.78
	OR3	-8.81	-0.03	-0.09	1.98	10.71	0.20
	OR4	-3.67	-1.72	0.00	2.18	10.01	0.39
	OR5	-4.77	4.02	-0.34	2.18	10.81	3.97

Table 1. Results force/torque measurements for Lesions 1 and 4.

Before conducting the experiment on Lesion 1 and Lesion 4, we apply the same procedure on a location at which there exists no lesion. The resulting display shows no peak. Examining the graphical displays in Figure 9 and 10 in comparison with that of the case of no lesion, we notice that a peak consistently occurs in the display. We can draw a preliminary conclusion here that a peak in the graphical display indicates the existence of a lesion.

In addition, the force and torque that we recorded in conjunction with the tactile sensing during palpation can give us the information about the contact location and how much force that we apply on the hard lump in the breast model.

4. Discussion and Conclusion

This paper has concerned with the detection of lumps in breast palpation using a tactile mapping device (TMD) system. It presented the main components of the TMD and explained their operations. Experiments were conducted on a breast model to detect two different types of lumps. Experimental data showed that the peak in the display of pressure distribution of the TMD indicated the presence of a lump. With the proven power of nonlinear signal processing using both convolution neural networks (CNN) and multi-layer perceptron (MLP), we expect that the tactile parameters associated with the lesions (i.e., the size and depth of the lesion) can be estimated more accurately than those by the conventional approaches using the first principle of engineering [6].